Int. J. Solids Structures Vol. 30, No. 12, pp. 1631–1648, 1993
Printed in Great Britain

0020–7683/93 $6.00+ .00
© 1993 Pergamon Press Ltd

DYNAMIC PLASTIC RESPONSE AND FAILURE OF A CLAMPED BEAM STRUCK TRANSVERSELY BY A MASS

WEI QIN SHEN† and NORMAN JONES
Impact Research Centre, Department of Mechanical Engineering, The University of Liverpool, PO Box 147, Liverpool L69 3BX, U.K.

(*Received* 7 *April* 1992; *in revised form* 16 *December* 1992)

Abstract—A theoretical analysis is presented which examines the dynamic response of a rigid–perfectly plastic clamped beam struck transversely by a mass at any point on the span. The analysis employs an interaction yield surface which combines the bending moment, membrane force and transverse shear force required for plastic flow. Material strain rate sensitive effects are examined with the aid of the Cowper–Symonds equation. Good agreement is obtained between the theoretical predictions for the maximum permanent transverse displacements and the corresponding experimental results. An energy density failure criterion is used to predict the dynamic inelastic failure of this impact problem.

NOMENCLATURE

q	material constant in eqn (51)
t	time
t_1, t_2	times at the ends of phases 1 and 2, respectively
t_f	time when motion ceases
$\dot{u}$	axial velocity at the impact point of a beam
A_f	smallest final cross-sectional area of a tensile specimen
A_o	original cross-sectional area of a tensile specimen
B	beam breadth
D	material constant in eqn (51)
E_l	plastic work dissipated in a plastic hinge at the left-hand side of the impact point
E_l^*	E_l/M_{do}
E_{ls}^*	dimensionless plastic shear work dissipated in a plastic hinge at the left-hand side of the impact point
G	mass of a striker
G^*	$G/(2\rho BHL)$
H	beam thickness
L	half length of a beam
M	bending moment
M_B, M_C	bending moments at the supports B and C, respectively
M_{do}	dynamic fully plastic bending moment
M_l, M_r	bending moments at the left- and right-hand sides of the impact point, respectively
M^*	M/M_{do}
N	membrane force
N_{do}	dynamic fully plastic membrane force
N^*	N/N_{do}
Q	transverse shear force
Q_B, Q_C	transverse shear forces at the supports B and C, respectively
Q_{do}	dynamic fully plastic transverse shear force
Q_l, Q_r	transverse shear forces at the left- and right-hand sides of the impact point, respectively
Q^*	Q/Q_{do}
S	location of the impact point from the left-hand support
S^*	S/L
V_o	initial velocity of a striker
W	transverse displacements at the left- and right-hand sides of the impact point during phase 1
W_A	transverse displacement at the impact point
W_B, W_C	transverse displacements at the supports B and C, respectively
W_l, W_r	transverse displacements at the left- and right-hand sides of the impact point, respectively
W_f	maximum permanent transverse displacement
W^*	W/H
α	length of a plastic hinge/H
β	E_{ls}^*/E_l^*
γ	$\sigma_{do}/(2\rho L^2)$
δ	$\sqrt{3}H/(2L)$
ε_c	critical strain

† Current address: The School of Systems Engineering, The University of Portsmouth, Portsmouth, U.K.

ε_f	rupture strain
ε_{mc}	maximum value of ε_c
$\dot{\varepsilon}_m$	mean strain rate
$\dot{\theta}_l$	angular velocity of the left-hand part of a beam
λ	$GV_o^2L/(2BH^3\sigma_o)$
ν	γ/δ
ξ	location of a travelling plastic hinge
ξ_o	initial location of a travelling plastic hinge
ξ^*	ξ/L
ρ	density of material
$\sigma_d(\varepsilon)$	dynamic stress–strain curve in a uniaxial tensile test
σ_{do}	dynamic yield stress
σ_o	static yield stress in a uniaxial tensile specimen
$\dot{\Delta}$	increment of axial elongation of a beam at the left- and right-hand sides of the impact point during phase I
$\dot{\Delta}_B, \dot{\Delta}_C, \dot{\Delta}_D$	increments of axial elongations of a beam at the supports B and C and at the location D, respectively
$\dot{\Delta}_l, \dot{\Delta}_r$	increments of axial elongations of a beam at the left- and right-hand sides of the impact point, respectively
$\dot{\Delta}^*$	$\dot{\Delta}/L$
ΔE_I	increment of plastic work for a time step Δt
ΔE_I^*	$\Delta E_I/M_{do}$
ΔE_{Is}^*	dimensionless increment of plastic shear work for a time step Δt
Δt	time step
Ω	density of plastic work dissipated at a plastic hinge in a beam
Ω^*	Ω/σ_{do}
Ω_c^*	dimensionless critical density of plastic work
$\dot{(\ )}$	$\partial(\ )/\partial t$
$\ddot{(\ )}$	$\partial^2(\ )/\partial t^2$.

1. INTRODUCTION

The dynamic plastic response of a fully clamped beam struck transversely by a mass at the centre or at any point on the span has been examined by several authors. Parkes (1958) studied the beam impact problem and developed a theoretical rigid, perfectly plastic analysis with travelling plastic bending hinges. However, this analysis was derived for infinitesimal displacements and, therefore, did not retain the influence of membrane forces in the yield condition, which would be important for transverse deflections larger than the beam thickness, approximately. Transverse shear forces were also neglected, but they would be important when the impact position is close to a support. Parkes' model was extended further by Nonaka (1967) who considered the influence of membrane forces on the behaviour of beams subjected to impacts at the mid-span which caused finite transverse deflections. A parabolic bending moment–membrane force yield curve is employed by Nonaka (1967), which is a unique yield curve in the M–N plane for a beam with a rectangular cross-section made from a perfectly plastic material (Shen and Jones, 1991a). It is shown by Shen and Jones (1991b) that the static admissibility of the extended Parkes' model in Nonaka (1967) is only violated slightly when the beam is struck by a heavy mass travelling at a low speed. The influence of the rotatory inertia and the transverse shear force on the response of a beam impacted at the mid-span is examined in Jones and de Oliveira (1979) and de Oliveira (1982) when plastic flow is controlled by a square M–Q yield condition. It is concluded in these two papers that rotatory inertia does not have a significant effect on the response but that the transverse shear force has a much more important influence. The dynamic response of a beam with a non-central impact is examined by Liu and Jones (1988) when plastic flow of the material is controlled by either M–N or M–Q square yield curves. No strain rate sensitivity is considered in any of the above analyses, except a simple estimate is made by Liu and Jones (1987).

It is evident from the experimental work by Liu and Jones (1987) and Yu and Jones (1991) that membrane forces dominate the behaviour of the beams with impacts near to the mid-span which produce transverse deflections larger than about one beam thickness. However, the membrane forces still play an important role when the impact point is close to a support, although the transverse shear forces contribute significantly to the response in this case, as shown in figures 26(a) and 27(a) in Liu and Jones (1987). Thus, an interaction yield surface, which was suggested by Shen and Jones (1991a) and Sobotka (1955) and

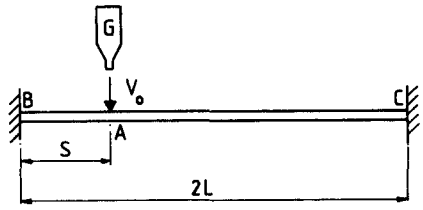

Fig. 1. A fully clamped beam struck transversely by a mass at a distance S from the left-hand support.

which combines the influences of the bending moment, axial tensile force and the transverse shear force, is necessary for predicting the response of this dynamic problem, as noted in Shen and Jones (1992) for a beam subjected to a uniformly distributed impulsive load.

The average strain rate obtained in this study for the beams tested by Liu and Jones (1987) and Yu and Jones (1991) is about 40 s^{-1}. Thus, the flow stress of the strain rate sensitive mild steel beams will be enhanced significantly, while the yield stress of the aluminium alloy beams will be less affected. The influence of material strain rate sensitivity is taken into account in this study with the aid of the Cowper–Symonds constitutive relation (Symonds, 1965; Jones, 1989a).

A theoretical analysis for the dynamic plastic response of a rigid–plastic clamped beam struck by a mass at any point on the span is presented in the next section. This analysis caters for the influence of finite transverse displacements and assumes that plastic yielding is controlled by the simultaneous influence of the bending moment, membrane force and the transverse shear force together with the strengthening influence of material strain rate sensitivity. The numerical predictions together with previously published experimental results are compared in Section 3. The failure of some of the specimens is examined in Section 4 with an energy density failure criterion, which was introduced earlier by the authors for beams loaded impulsively.

2. DYNAMIC RESPONSE OF A CLAMPED BEAM UNDER IMPACT LOADING

The fully clamped beam in Fig. 1 has a length $2L$, width B, thickness H and a mass density ρ, and is struck by a mass G travelling with an initial velocity V_0 at a point A which is a distance S ($S < L$) from the left-hand support. After impact, the striker G is assumed to remain in contact with the beam. Therefore, the striker and the struck point of the beam have an initial velocity V_0 at the instant of contact and a common velocity throughout the entire response.†

The plastic yielding of the beam in Fig. 1 is controlled by an interaction yield condition which is expressed in terms of the bending moment M, axial tensile force N and the transverse shear force Q in the form (Sobotka, 1955)

$$|M^*|\sqrt{1-Q^{*2}}+N^{*2}+Q^{*2}=1, \tag{1}$$

as shown in Fig. 2, where $M^* = M/M_{do}$, $Q^* = Q/Q_{do}$ and $N^* = N/N_{do}$. N is assumed to remain constant along the length of a beam since the influence of axial inertia is small enough to be neglected. The quantities $M_{do} = \sigma_{do}BH^2/4$, $Q_{do} = \sigma_{do}BH/\sqrt{3}$ and $N_{do} = \sigma_{do}BH$ are the fully plastic bending moment, transverse shear force and membrane force, respectively, for a beam which is made from a rigid, perfectly plastic strain rate sensitive material with a dynamic flow stress σ_{do}. Equation (1) is shown to be statically admissible by Shen and Jones (1991a).

† Most of the initial kinetic energy of a striker is dissipated by plastic deformations in a beam, particularly when the mass of a striker is much larger than the beam mass. However, some rebounding of a striker was observed in all of the experimental tests reported by Liu and Jones (1987) and Yu and Jones (1991), except those which ruptured.

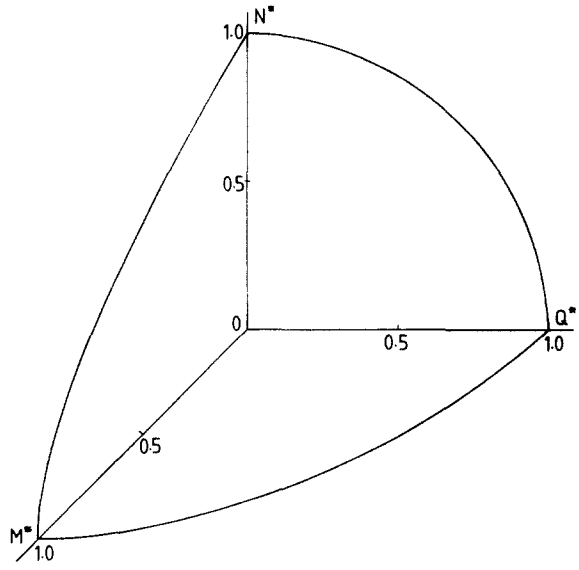

Fig. 2. An interaction yield surface (Shen and Jones, 1991a; Sobotka, 1955).

There are three phases of motion during the entire response for the asymmetric impact problem in Fig. 1. The response durations for the first and second phases of motion with both travelling and stationary plastic hinges are short when the mass ratio (G^*) is large. In this case, most of the transverse deflection is accumulated and the plastic work is dissipated during the third phase of motion which has only stationary plastic hinges.

2.1. *Phase* 1: $0 \leqslant t < t_1$

It is assumed that a stationary plastic hinge develops at the impact point together with two travelling hinges which form at the two points $\xi = \xi_0$ ($\xi_0 \neq 0$) and move symmetrically with respect to the impact point towards the supports, as shown in Fig. 3(a).

The yield curve for the fully clamped support B is

$$M_B^* + N^{*2} = 1, \tag{2}$$

which corresponds to the $Q^* = 0$ plane in Fig. 2.

The transverse equilibrium equations for the impact point and the region AB, together with the moment equilibrium equation for the region AB, are

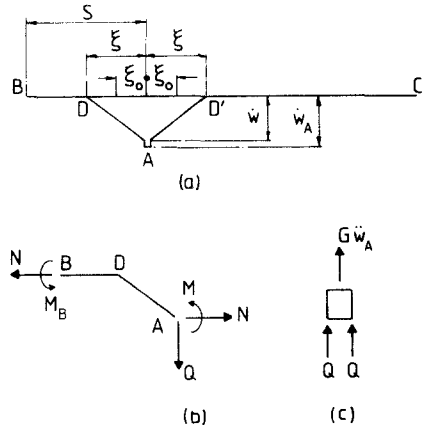

Fig. 3. Phase 1. (a) Velocity profile. (b) Generalized forces and moments. (c) Dynamic forces on striker.

$$G\ddot{W}_A+2Q=0, \tag{3}$$

$$\frac{\mathrm{d}}{\mathrm{d}t}(\rho BH\xi\dot{W}/2)=Q \tag{4}$$

and

$$\frac{\mathrm{d}}{\mathrm{d}t}(\rho BH\xi^2\dot{W}/6)=M_B+M+NW, \tag{5}$$

respectively. Equations (3)–(5) are rewritten in the form

$$G^*\ddot{W}_A^*=-vQ^*, \tag{3}'$$

$$\frac{\mathrm{d}}{\mathrm{d}t}(\dot{W}^*\xi^*)=2vQ^* \tag{4}'$$

and

$$\frac{\mathrm{d}}{\mathrm{d}t}(\dot{W}^*\xi^{*2})=3\gamma[(M_B^*+M^*)+4N^*W^*], \tag{5}'$$

where $G^*=G/(2\rho BHL)$, $\gamma=\sigma_{do}/(2\rho L^2)$, $\delta=\sqrt{3H/(2L)}$, $v=\gamma/\delta$. $\xi^*=\xi/L$ and $W^*=W/H$.

The normality requirement of plasticity for the transverse velocity profile in Fig. 3(a) and the yield condition in Fig. 2 demands that

$$\frac{\dot{W}_A-\dot{W}}{\dot{W}/\xi}=-\frac{\mathrm{d}M}{\mathrm{d}Q}, \tag{6}$$

$$\frac{\dot{\Delta}}{\dot{W}/\xi}=-\frac{\mathrm{d}M}{\mathrm{d}N} \tag{7}$$

and

$$\frac{\dot{\Delta}_D}{\dot{W}/\xi}=-\frac{\mathrm{d}M_B}{\mathrm{d}N}, \tag{8}$$

where $\dot{\Delta}$ and $\dot{\Delta}_D$ are the increments of the axial elongation at the left-hand side of point A and the right-hand side of point D in Fig. 3(a), respectively. With eqns (1) and (2), eqns (6)–(8) yield

$$\frac{(\dot{W}_A^*-\dot{W}^*)\xi^*}{\dot{W}^*}=\tfrac{1}{2}\delta Q^*(2-M^*/\sqrt{1-Q^{*2}})/\sqrt{1-Q^{*2}}, \tag{6}'$$

$$\frac{\dot{\Delta}^*\xi^*}{\dot{W}^*}=\tfrac{2}{3}\delta^2N^*/\sqrt{1-Q^{*2}} \tag{7}'$$

and

$$\frac{\dot{\Delta}_D^*\xi^*}{\dot{W}^*}=\tfrac{2}{3}\delta^2N^*, \tag{8}'$$

respectively, where $\dot{\Delta}^*=\dot{\Delta}/L$. By means of the approximate geometric relation

$$\dot{\Delta}+\dot{\Delta}_D\cong W\dot{W}/\xi, \tag{9}$$

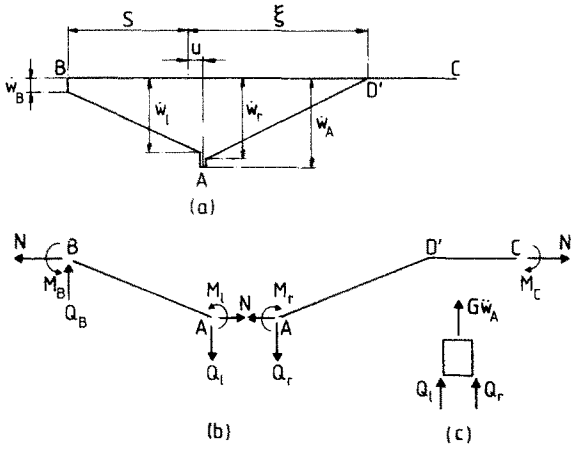

Fig. 4. Phase 2. (a) Velocity profile. (b) Generalized forces and moments. (c) Dynamic forces on striker.

or

$$\dot{\Delta}^* + \dot{\Delta}_D^* \cong \tfrac{4}{3}\delta^2 W^* \dot{W}^*/\xi^*, \tag{9}'$$

eqns (7)′–(9)′ give

$$W^* = \tfrac{1}{2}N^*(1 + 1/\sqrt{1-Q^{*2}}). \tag{10}\dagger$$

The complete solution at any time during the first phase of motion may be obtained by solving eqns (1)–(2), (3)′–(6)′ and (10) by means of the well-known Runge–Kutta method with the initial conditions:

$$W = 0, \quad \dot{W} = 0, \quad W_A = 0, \quad \dot{W}_A = V_0,$$
$$N^* = 0, \quad M^* = 0, \quad Q^* = 1, \quad M_B^* = 1 \quad \text{and} \quad \xi_0 > 0$$

at $t = 0$. A time step of 10^{-8} s is used in the calculations. Phase 1 ends at $t = t_1$ when $\xi = S$ and the values of the variables at $t = t_1$ are the initial conditions for the next phase of motion. If $\xi_0 > S$, then no phase 1 occurs and different initial conditions are required for phase 2, as discussed later.

2.2. *Phase* 2: $t_1 \leqslant t < t_2$

The left-hand travelling plastic hinge reaches the support B at $t = t_1$ where it remains throughout this phase of motion. However, the right-hand travelling hinge continues to move towards the support C, as shown in Fig. 4, where u is the axial displacement of the impact point A.

The yield conditions for the points B, C and the left- and right-hand sides of point A in Fig. 4 are

$$M_B^*\sqrt{1-Q_B^{*2}} + N^{*2} + Q_B^{*2} = 1, \tag{11}$$

$$M_C^* + N^{*2} = 1, \tag{12}$$

$$M_l^*\sqrt{1-Q_l^{*2}} + N^{*2} + Q_l^{*2} = 1 \tag{13}$$

† Equation (10) with $Q^* = 0$ gives $W^* = N^*$ which predicts that $W^* = 1$ when $N^* = 1$, as noted by Jones (1989a) for a static concentrated load acting at the mid-span of a fully clamped beam.

and

$$M_r^*\sqrt{1-Q_r^{*2}}+N^{*2}+Q_r^{*2}=1, \tag{14}$$

respectively.

The transverse equilibrium equations for the impact point and for the segments AB and AD' are

$$G\ddot{W}_A+Q_l+Q_r=0, \tag{15}$$

$$\frac{d}{dt}[\rho BHS(\dot{W}_l+\dot{W}_B)/2]=Q_l-Q_B \tag{16}$$

and

$$\frac{d}{dt}[\rho BH\xi\dot{W}_r/2]=Q_r, \tag{17}$$

respectively. The moment equilibrium equations for the regions AB and AD' are

$$\frac{d}{dt}\left[\rho BHS\frac{\dot{W}_l+\dot{W}_B}{2}\frac{S}{2}-\frac{1}{12}\rho BH(\dot{W}_l-\dot{W}_B)S^2\right]\cong N(W_l-W_B)-Q_BS+M_B+M_l \tag{18}$$

and

$$\frac{d}{dt}[\rho BH\xi^2\dot{W}_r/6]\cong NW_r+M_C+M_r, \tag{19}$$

respectively. The approximations $S+u\approx S$ and $\xi-u\approx\xi$ are used in deriving eqns (16)–(19) since u is small compared with S and ξ. Equations (15)–(19) give

$$G^*\ddot{W}_A^*=-v(Q_l^*+Q_r^*)/2, \tag{15}'$$

$$\ddot{W}_B^*=[-2vS^*(Q_l^*+2Q_B^*)+3\gamma(M_B^*+M_l^*)+12\gamma N^*(W_l^*-W_B^*)]/S^{*2}, \tag{20}$$

$$\ddot{W}_l^*=[2vS^*(2Q_l^*+Q_B^*)-3\gamma(M_B^*+M_l^*)-12\gamma N^*(W_l^*-W_B^*)]/S^{*2}, \tag{21}$$

$$\ddot{W}_r^*=[4v\xi^*Q_r^*-3\gamma(M_C^*+M_r^*)-12\gamma N^*W_r^*]/\xi^{*2} \tag{22}$$

and

$$\dot{\xi}^*=[-2v\xi^*Q_r^*+3\gamma(M_C^*+M_r^*)+12\gamma N^*W_r^*]/(\xi^*\dot{W}_r^*), \tag{23}$$

respectively, where $S^*=S/L$.

The normality principle of plasticity associated with the yield conditions (11)–(14) and Fig. 2 requires that

$$\frac{\dot{W}_B}{(\dot{W}_l-\dot{W}_B)/S}\cong-\frac{dM_B}{dQ_B}, \tag{24}$$

$$\frac{\dot{\Delta}_B}{(\dot{W}_l-\dot{W}_B)/S}\cong-\frac{dM_B}{dN}, \tag{25}$$

$$\frac{\dot{W}_A-\dot{W}_l}{(\dot{W}_l-\dot{W}_B)/S}\cong-\frac{dM_l}{dQ_l}, \tag{26}$$

$$\frac{\dot{\Delta}_l}{(\dot{W}_l-\dot{W}_B)/S}\cong-\frac{dM_l}{dN}, \tag{27}$$

$$\frac{\dot{W}_A - \dot{W}_r}{\dot{W}_r/\xi} \cong -\frac{dM_r}{dQ_r}, \tag{28}$$

$$\frac{\dot{\Delta}_r}{\dot{W}_r/\xi} \cong -\frac{dM_r}{dN} \tag{29}$$

and

$$\frac{\dot{\Delta}_C}{\dot{W}_r/\xi} \cong -\frac{dM_C}{dN}, \tag{30}$$

where $\dot{\Delta}_B$, $\dot{\Delta}_l$, $\dot{\Delta}_r$ and $\dot{\Delta}_C$ are defined similarly to $\dot{\Delta}$ in Section 2.1.

Geometric compatibility provides the approximate expressions

$$\dot{\Delta}_B + \dot{\Delta}_l \cong \dot{u} + (W_l - W_B)(\dot{W}_l - \dot{W}_B)/S \tag{31}$$

and

$$\dot{\Delta}_C + \dot{\Delta}_r \cong -\dot{u} + W_r \dot{W}_r/\xi. \tag{32}$$

Using the yield conditions expressed by eqns (11)–(14), eqns (24)–(32) are recast into the form

$$\frac{\dot{W}_B^* S^*}{\dot{W}_l^* - \dot{W}_B^*} \cong \tfrac{1}{2}\delta Q_B^*(2 - M_B^*/\sqrt{1-Q_B^{*2}})/\sqrt{1-Q_B^{*2}}, \tag{24}'$$

$$\frac{(\dot{W}_A^* - \dot{W}_l^*)S^*}{\dot{W}_l^* - \dot{W}_B^*} \cong \tfrac{1}{2}\delta Q_l^*(2 - M_l^*/\sqrt{1-Q_l^{*2}})/\sqrt{1-Q_l^{*2}}, \tag{26}'$$

$$\frac{(\dot{W}_A^* - \dot{W}_r^*)\xi^*}{\dot{W}_r^*} \cong \tfrac{1}{2}\delta Q_r^*(2 - M_r^*/\sqrt{1-Q_r^{*2}})/\sqrt{1-Q_r^{*2}}, \tag{28}'$$

$$W_l^* - W_B^* + \frac{\sqrt{3}}{2\delta}\frac{\dot{u}^* S^*}{\dot{W}_l^* - \dot{W}_B^*} \cong \tfrac{1}{2}N^*(1/\sqrt{1-Q_B^{*2}} + 1/\sqrt{1-Q_l^{*2}}) \tag{33}$$

and

$$W_r^* - \frac{\sqrt{3}}{2\delta}\frac{\dot{u}^* \xi^*}{\dot{W}_r^*} \cong \tfrac{1}{2}N^*(1 + 1/\sqrt{1-Q_r^{*2}}), \tag{34}$$

where $\dot{u}^* = \dot{u}/H$.

Equations (11)–(14), (15)′, (20)–(23), (24)′, (26)′, (28)′ and (33)–(34) are solved using the Runge–Kutta method with the time step of 10^{-8} s to provide

$$W_l, \dot{W}_l, W_r, \dot{W}_r, W_A, \dot{W}_A, W_B, \dot{W}_B, N, Q_l, M_l, Q_r, M_r, Q_B, M_B, M_C \text{ and } \xi$$

during this phase of motion which ends at $t = t_2$ when $\xi = 2L - S$.

If $\xi_o > S$, then no phase 1 occurs, as mentioned in Section 2.1, and the beam motion commences at phase 2 with the following initial conditions:

$$W_l = 0, \quad \dot{W}_l = 0, \quad W_r = 0, \quad \dot{W}_r = 0, \quad W_A = 0, \quad \dot{W}_A = V_o, \quad W_B = 0, \quad \dot{W}_B = 0,$$
$$N^* = 0, \quad Q_l^* = 1, \quad M_l^* = 0, \quad Q_r^* = 1, \quad M_r^* = 0, \quad Q_B^* > 0, \quad M_B^* < 1, \quad M_C^* = 1$$
$$\text{and } \xi_o > S \text{ at } t = 0.$$

The initial values of Q_B^* and M_B^* are determined from

$$\frac{\delta}{S^*}\frac{Q_B^*}{\sqrt{1-Q_B^{*2}}}-\frac{3\gamma\sqrt{1-Q_B^{*2}}-2\beta S^*(1+2Q_B^*)}{3\beta S^*(1+Q_B^*)-3\gamma\sqrt{1-Q_B^{*2}}}=0 \tag{35}$$

and

$$M_B^*=\sqrt{1-Q_B^{*2}}, \tag{36}$$

which are derived from eqns (20)–(21) and (24)′, and $N^*=0$ at $t=0$.

Phase 2 ends at $t=t_2$ when the right-hand travelling plastic hinge reaches the support C. The values of the variables at $t=t_2$ are the initial conditions for the next phase of motion.

2.3. *Phase* 3: $t_2 \leqslant t \leqslant t_f$

After the right-hand travelling hinge reaches the support C, the beam continues to deform with the transverse velocity profile shown in Fig. 5.

The yield condition for point C is

$$M_C^*\sqrt{1-Q_C^{*2}}+N^{*2}+Q_C^{*2}=1. \tag{37}$$

It is evident that eqns (15)′ and (20)–(21) can be used in this phase of motion, and that $\ddot{W}_C^*$ and $\ddot{W}_r^*$ are the same as $\ddot{W}_B^*$ and $\ddot{W}_l^*$, respectively, except for S^* being replaced by $2-S^*$ and changing the subscripts l and B into r and C, respectively. Thus

$$\ddot{W}_C^*=[-2v(2-S^*)(Q_r^*+2Q_C^*)+3\gamma(M_C^*+M_r^*)+12\gamma N^*(W_r^*-W_C^*)]/(2-S^*)^2 \tag{38}$$

and

$$\ddot{W}_r^*=[2v(2-S^*)(2Q_r^*+Q_C^*)-3\gamma(M_C^*+M_r^*)-12\gamma N^*(W_r^*-W_C^*)]/(2-S^*)^2. \tag{39}$$

Similarly, eqns (24)′, (26)′ and (33) are required for normality during this phase of motion and give

$$\frac{\dot{W}_C^*(2-S^*)}{\dot{W}_r^*-\dot{W}_C^*}\cong\tfrac{1}{2}\delta Q_C^*(2-M_C^*/\sqrt{1-Q_C^{*2}})/\sqrt{1-Q_C^{*2}}, \tag{40}$$

$$\frac{(\dot{W}_A^*-\dot{W}_r^*)(2-S^*)}{(\dot{W}_r^*-\dot{W}_C^*)}\cong\tfrac{1}{2}\delta Q_r^*(2-M_r^*/\sqrt{1-Q_r^{*2}})/\sqrt{1-Q_r^{*2}}, \tag{41}$$

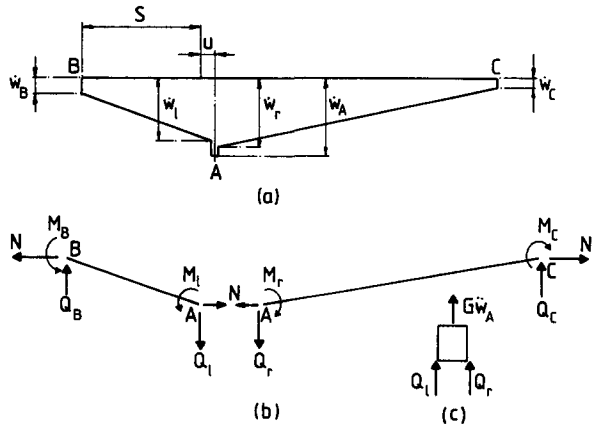

Fig. 5. Phase 3. (a) Velocity profile. (b) Generalized forces and moments. (c) Dynamic forces on striker.

$$W_r^* - W_C^* - \frac{\sqrt{3}}{2\delta}\frac{\dot{u}^*(2-S^*)}{\dot{W}_r^* - \dot{W}_C^*} \cong \tfrac{1}{2}N^*(1/\sqrt{1-Q_C^{*2}} + 1/\sqrt{1-Q_r^{*2}}). \tag{42}$$

This phase of motion ends when the motion of a beam ceases at $t = t_f$.

2.4. *Dissipation of plastic work*

Attention is focused only on the largest dissipation of plastic work E_1 which occurs at the left-hand side of the impact point. The increment of total plastic work ΔE_1 for every time step Δt is

$$\Delta E_1 = [M_1\dot{\theta}_1 + Q_1(\dot{W}_A - \dot{W}_1) + N\dot{\Delta}_1]\,\Delta t, \tag{43}$$

where $\dot{\theta}_1$ is the angular velocity associated with M_1, i.e.

$$\dot{\theta}_1 = \dot{W}/\xi, \qquad \text{for phase 1}$$

and

$$\dot{\theta}_1 = (\dot{W}_1 - \dot{W}_B)/S, \quad \text{for phases 2 and 3.}$$

The dimensionless form of eqn (43) is

$$\Delta E_1^* = \frac{\Delta E_1}{M_{do}} = \left[M_1^*\dot{\theta}_1 + \frac{4}{\sqrt{3}}Q_1^*(\dot{W}_A^* - \dot{W}_1^*) + \frac{2\sqrt{3}}{\delta}N^*\dot{\Delta}_1^*\right]\Delta t, \tag{43}'$$

while the dissipation of plastic shear work at the left-hand side of the impact point is

$$\Delta E_{1s}^* = \frac{4}{\sqrt{3}}Q_1^*(\dot{W}_A^* - \dot{W}_1^*)\,\Delta t. \tag{44}$$

Thus

$$E_1^* = \Sigma\,\Delta E_1^* \tag{45}$$

and

$$E_{1s}^* = \Sigma\,\Delta E_{1s}^*. \tag{46}$$

Now, the ratio

$$\beta = \frac{E_{1s}^*}{E_1^*} \tag{47}$$

was introduced by Shen and Jones (1992) so that the empirical formula

$$\alpha + 1.2\beta = 1.3, \tag{48}$$

which was used to relate the length of a plastic hinge αH to the parameter β for impulsively loaded beams may be used for the current impact problem.

The total plastic energy density at a plastic hinge is taken as

$$\Omega = \frac{E_1}{\alpha H^2 B} = \frac{E_1^*\sigma_{do}}{4\alpha},$$

the dimensionless form of which is

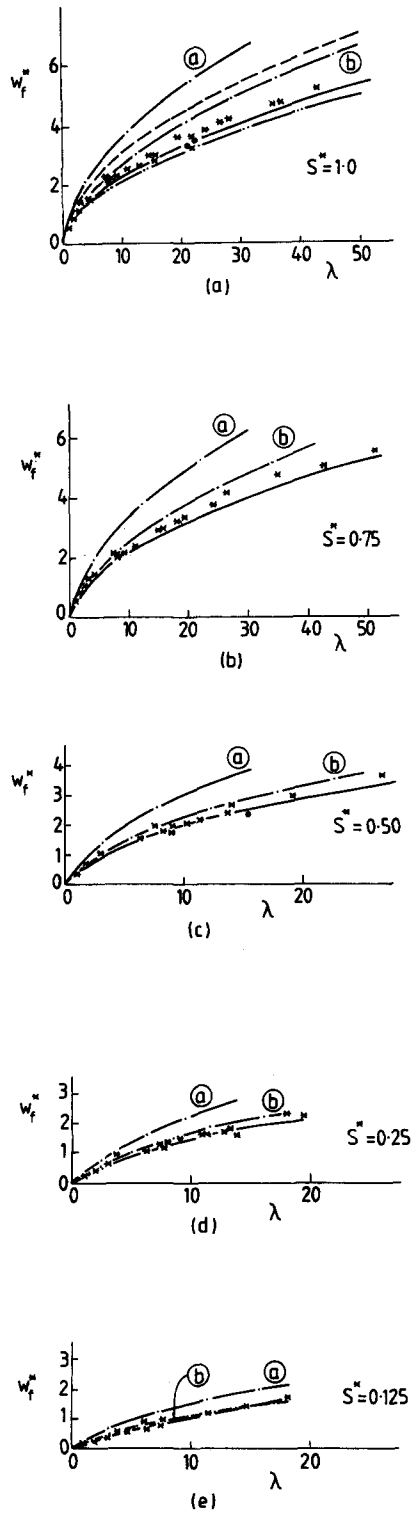

Fig. 6. Variation of the dimensionless displacement W_f^* with λ for mild steel beams with $\rho = 7860$ kg m^{-3}, $L = 50.8$ mm, $B = 10.16$ mm and $\sigma_0 = 337$ N mm^{-2} for the $H = 3.81$ and 5.08 mm specimens and $\sigma_0 = 302$ N mm^{-2} for the $H = 6.35$ and 7.62 mm specimens in Liu and Jones (1987) and $\sigma_0 = 264$ N mm^{-2} for the $H = 6.24$ mm specimens in Yu and Jones (1991) struck by a mass of 5 kg. * Experimental results from Liu and Jones (1987). ○ Experimental results from Yu and Jones (1991). ———— Present theoretical predictions with $D = 40$ s^{-1} and $q = 5$. — — — — — Nonaka (1967) for a strain rate insensitive material. ——·—— Theoretical predictions from Liu and Jones (1988) for a strain rate insensitive material; (a)—upper bound, (b)—lower bound. ——··—— Modified Nonaka's curve with $D = 40$ s^{-1} and $q = 5$. (a) $S^* = 1.0$. (b) $S^* = 0.75$. (c) $S^* = 0.5$. (d) $S^* = 0.25$. (e) $S^* = 0.125$.

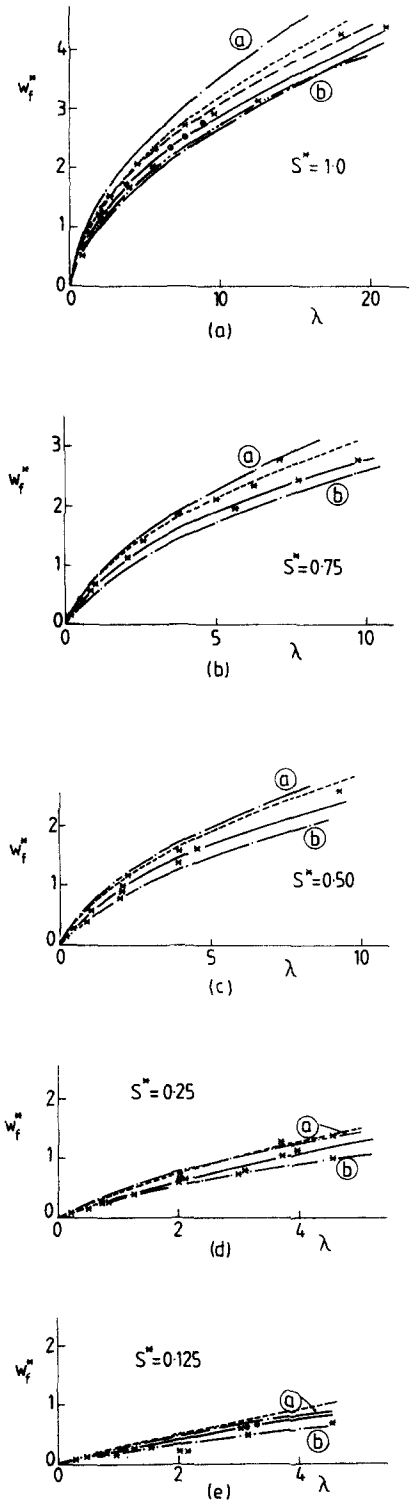

Fig. 7. Variation of the dimensionless displacement W_f^* with λ for aluminium alloy beams with $\rho = 2700$ kg m^{-3}, $L = 50.8$ mm, $B = 10.16$ mm and $\sigma_o = 354.5$ N mm^{-2} for the $H = 3.81$, 5.08 and 6.35 mm specimens and $\sigma_o = 412$ N mm^{-2} for the $H = 7.62$ mm specimens in Liu and Jones (1987) and $\sigma_o = 207.5$ N mm^{-2} for the $H = 6.39$ mm specimens in Yu and Jones (1991) struck by a mass of 5 kg. * Experimental results from Liu and Jones (1987). ○ Experimental results from Yu and Jones (1991). ———— Present theoretical predictions with $D = 6500$ s^{-1} and $q = 4$. - - - - - - - - - Present theoretical predictions but neglecting strain rate effect. — — — — — Nonaka (1967) for a strain rate insensitive material. ——·—— Theoretical predictions from Liu and Jones (1988) for a strain rate insensitive material; a—upper bound, b—lower bound. ——··—— Modified Nonaka's curve with $D = 6500$ s^{-1} and $q = 4$. (a) $S^* = 1.0$. (b) $S^* = 0.75$. (c) $S^* = 0.5$. (d) $S^* = 0.25$. (e) $S^* = 0.125$.

$$\Omega^* = \frac{\Omega}{\sigma_{do}} = \frac{E_1^*}{4\alpha}. \tag{49}$$

Thus, the dimensionless critical energy density is

$$\Omega_c^* = \varepsilon_c, \tag{50}$$

where ε_c is a value of a strain which is to be determined when considering various factors in an actual structural problem.

The dynamic flow stress for a rigid, perfectly plastic material is taken in the form

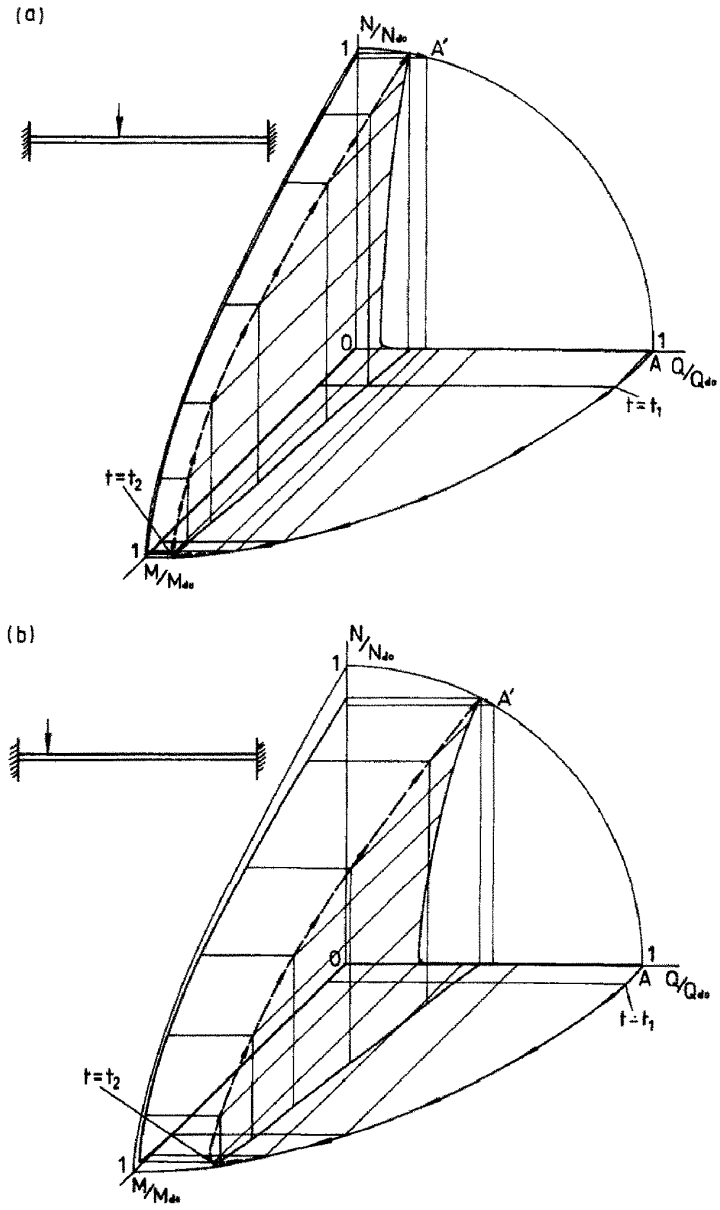

Fig. 8. Variation of the generalized stresses at the left-hand side of the impact point during the response of a fully clamped beam with $\rho = 7860$ kg m^{-3}, $L = 50.8$ mm, $B = 10.16$ mm, $H = 3.81$ mm in Liu and Jones (1987) struck by a mass of 5 kg travelling at an initial speed of 2.67 m s^{-1}. (a) $S^* = 0.75$. (b) $S^* = 0.25$. (c) $S^* = 0.125$. (d) $S^* = 0.1$.

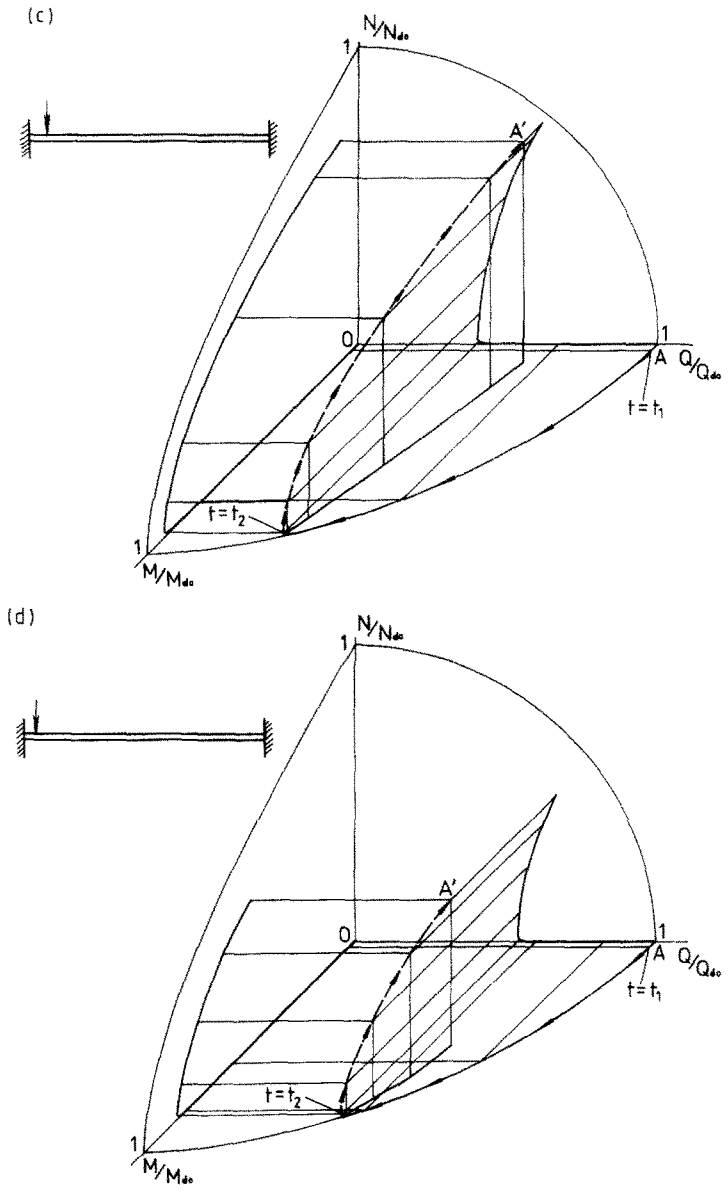

Fig. 8. *Continued.*

$$\sigma_{do} = \sigma_o\left[1+\left(\frac{\dot{\varepsilon}_m}{D}\right)^{1/q}\right], \tag{51}$$

according to the Cowper–Symonds constitutive equation (Symonds, 1965), where σ_o is the initial flow stress in a static uniaxial tensile test and D and q are material constants which are determined from dynamic tensile tests on the material. The values of D and q for several materials are listed by Jones (1989a). The term $\dot{\varepsilon}_m$ in eqn (51) is the mean uniaxial strain rate which is estimated from

$$\dot{\varepsilon}_m = \frac{\Omega^*}{t_f}, \tag{52}$$

and is obtained using an iterative procedure which is terminated when the difference between the dynamic flow stress in eqn (51) is less than 1%. The maximum value of ε_c is obtained from the expression

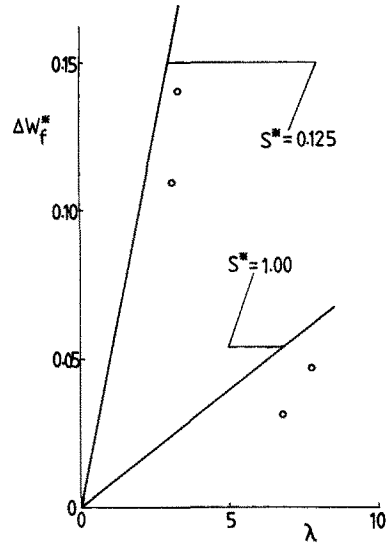

Fig. 9. Variation of ΔW_f^* with λ for the aluminium alloy beams in Yu and Jones (1991) with $\sigma_o = 207.5$ N mm^{-2}, $H = 6.39$ mm and $S^* = 1.0$ and $S^* = 0.125$. ———— Present theoretical predictions with $D = 6500$ s^{-1} and $q = 4$. ○ Experimental results from Yu and Jones (1991).

$$\varepsilon_{mc} = \frac{1}{\sigma_{do}} \int_0^{\varepsilon_f} \sigma_d(\varepsilon, \dot{\varepsilon}_m)\, d\varepsilon, \tag{53}$$

where $\sigma_d(\varepsilon, \dot{\varepsilon}_m)$ is the dynamic engineering stress–strain curve which is obtained from a dynamic uniaxial tensile test for a given strain rate $\dot{\varepsilon}_m$ and ε_f is the engineering rupture strain for a zero gauge length which is calculated from $\varepsilon_f = A_o/A_f - 1$, where A_o and A_f are the original and the smallest final cross-sectional areas of a tensile specimen, respectively. It is evident that Ω^* may be interpreted as the average strain in the most severely deformed plastic region of a beam.

3. RESULTS AND DISCUSSION

Figures 6 and 7, respectively, show the present theoretical predictions for the dimensionless final permanent transverse deflection W_f^* at the impact point versus the dimensionless initial kinetic energy parameter $\lambda = GV_o^2L/(2BH^3\sigma_o)$ for mild steel and aluminium alloy beams struck at five different positions. The strain rate sensitive behaviour of the mild steel beams is characterized by eqns (51) and (52) with $D = 40$ s^{-1} and $q = 5$ from Symonds (1965). Two sets of results are presented for the aluminium alloy beams. One set of curves is calculated for a strain rate insensitive material, while the other set uses eqns (51) and (52) with $D = 6500$ s^{-1} and $q = 4$ from Symonds (1965). For comparison purposes, the theoretical predictions of Nonaka (1967) are also shown in Figs 6(a) and 7(a), in which an exact parabolic M–N yield condition is used but the influence of strain rate sensitivity is disregarded. The authors of this paper have modified Nonaka's curves by replacing σ_o by σ_{do} which is calculated from eqn (51) using the values of $\dot{\varepsilon}_m$ estimated according to eqn (52). The theoretical predictions derived in Liu and Jones (1988) using square M–N yield curves, which inscribe and circumscribe the parabolic yield curve, and without retaining the influence of material strain rate sensitivity, are also drawn in Figs 6(a)–(e) and 7(a)–(e).

Surprisingly good agreement is observed at the five impact positions in Figs 6 and 7 between the present theoretical predictions and the experimental results for the mild steel and aluminium alloy specimens reported by Liu and Jones (1987) and Yu and Jones (1991). This agreement is achieved because the influences of finite deflections (i.e. membrane forces) and material strain rate sensitivity (which is especially important for mild steel) and the effect of the transverse shear force on yielding (which is particularly important when the impact point is close to the supports) are retained in the present study.

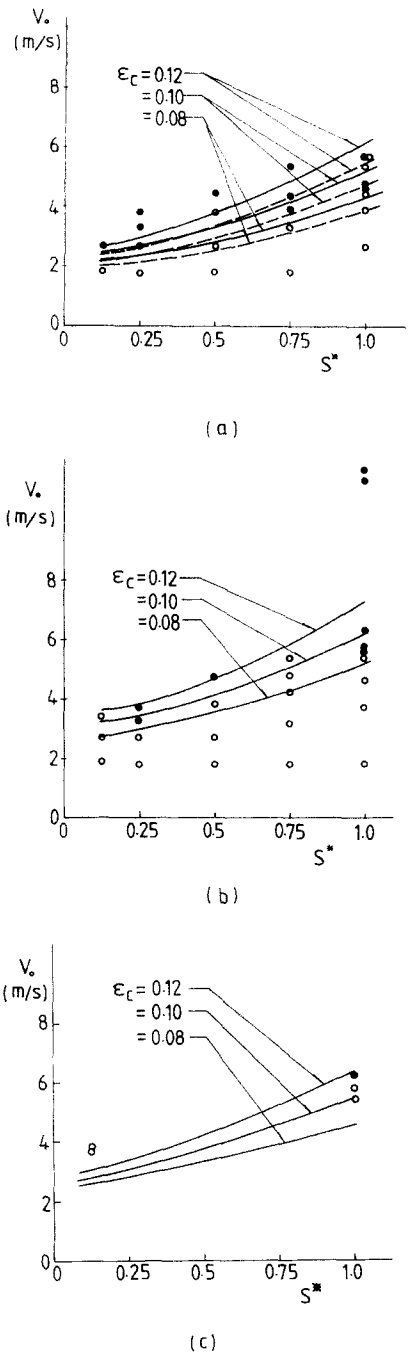

Fig. 10. Comparison between the present theoretical predictions with several values of ε_c for failure and the experimental results for the aluminium alloy beams in Liu and Jones (1987) and Yu and Jones (1991). ——— Present theoretical predictions with $D = 6500\ s^{-1}$ and $q = 4$. - - - - - Present theoretical predictions for a strain rate insensitive material. • Ruptured. ○ No failure. (a) $H = 3.81$ mm in Liu and Jones (1987). (b) $H = 5.08$ mm in Liu and Jones (1987). (c) $H = 6.39$ mm in Yu and Jones (1991).

The comparisons made in Fig. 6 reveal that the material strain rate sensitive properties must be considered for the mild steel specimens even for the low speed impacts. However, the comparisons between the present theoretical predictions in Fig. 7 with (———) and without (— — — — —) strain rate effects show that the influence of material strain rate sensitivity for the relatively strain rate insensitive aluminium alloy beams subjected to low speed impacts is not negligible although there is some doubt about the strain rate sensitive properties of some aluminium alloys (Jones, 1974). However, it has been noted in

Jones (1989b) that the strain rate sensitivity of some materials is greatest for small strains near the yield stress and is less significant for large plastic strains. A modified form of the Cowper–Symonds equation, which incorporates this phenomenon, is presented by Jones (1989b). Equation (51) does not cater for the variation of the material strain rate sensitivity with strain which could be particularly significant when estimating the rupture of beams. An equation which recognized this phenomenon was presented by Jones (1989b, c) but it has not been used in the present calculations because eqns (51) and (52) give a constant dynamic flow stress based on an average strain rate throughout the entire duration of a test which is a good approximation of the dynamic uniaxial tensile data.

Figures 8(a)–(d) show the variation of the transverse shear forces on the left-hand side of the impact point A for different locations of the striker on a beam span. The generalized stresses on the left-hand side of the impact point change from point A at initial impact along the dotted curves on the yield surface given by eqn (1) to point A' when motion ceases, as shown in Fig. 8. It transpires that the transverse shear force exercises a more important influence on plastic yielding when the impact point is located close to the supports. The small differences between the modified Nonaka's curves, which incorporated the influence of material strain rate sensitivity according to eqns (51) and (52) but neglected transverse shear effects, and the present theoretical predictions in Figs 6(a) and 7(a), which included both effects, indicate that the influence of the transverse shear force is not very important for impacts at the mid-span. However, it is observed that the differences between the mean values of the theoretical curves labelled "a" and "b" for the inscribing and circumscribing yield criteria (Liu and Jones, 1988), and the present theoretical predictions, decrease from Figs 6(a) to (e) and from Figs 7(a) to (e). This trend suggests, possibly, that the influence of the transverse shear force is more important for impact positions close to the supports. Figure 9 shows the variation of the dimensionless transverse shear displacements $\Delta W_f^* = W_A^* - W_f^*$ when $t = t_f$ with λ for the aluminium alloy beams which were tested by Yu and Jones (1991). A comparison between the two cases of $S^* = 1$ and $S^* = 0.125$ shows a strong influence of the transverse shear effects when the impact point is close to a support.

4. FAILURE PREDICTION

It is suggested by Shen and Jones (1992) that an energy density failure criterion may be used to predict the dynamic inelastic failure (rupture) of a structural component when $\Omega^* \geqslant \Omega_c^* = \varepsilon_c$ according to eqn (50) here.

A rupture strain of magnitude $\varepsilon_f = 0.5$† is selected as ε_c by Shen and Jones (1992) in order to predict the dynamic inelastic failure of impulsively loaded aluminium alloy 6061 T6 beams having a breadth of 25.4 mm and thicknesses of 4.75–9.53 mm. However, the appropriate value of ε_c might be much lower than the value of ε_f for the beams examined by Liu and Jones (1987) and Yu and Jones (1991), since a local impact loading may induce local deformations which reduce the strength of the beam. Moreover, the rupture strain of materials may change with strain rate, as discussed further by Jones (1989b, c).

The experimental results for the failure of the aluminium alloy beams, which were reported by Liu and Jones (1987) and Yu and Jones (1991) for thicknesses of 3.81, 5.08 and 6.39 mm, are shown in Figs 10(a)–(c), respectively. Theoretical curves from the present study are also presented in Figs 10(a)–(c) for the threshold values of the initial velocities that would cause rupture of the beams for different values of ε_c, where the strain rate effects are examined at the different velocities using $D = 6500\ s^{-1}$ and $q = 4$. The comparisons in Figs 10(a) and 10(b) reveal that the theoretical predictions with ε_c between 0.08 and 0.12

† An engineering rupture strain of 0.66 (average of 0.529 and 0.785) is reported by Yu and Jones (1991) for an aluminium alloy material at a strain rate of 140 s^{-1} and having a nominal static ($\dot{\varepsilon} = 0.0012\ s^{-1}$) rupture strain of 0.176 (average of 0.160, 0.188 and 0.181). Thus, the engineering rupture strain at a high strain rate is estimated in Shen and Jones (1992) as $\varepsilon_f = 0.66 \times 0.135/0.176 = 0.50$ for the aluminium alloy 6061 T6 having a nominal static rupture strain of 0.135. This estimate is made in the absence of an experimental value and is approximate because the engineering rupture strain of many materials is a non-linear function of strain rate, as remarked by Jones (1989b).

would bound the experimental results for the dynamic inelastic failure of the aluminium alloy beams in Liu and Jones (1987).

It appears that the value of ε_c to be used in eqn (50) for the dynamic inelastic failure of structures is related strongly to the actual geometric characteristics of a structural member, as well as the material properties.

5. CONCLUSIONS

A theoretical rigid–plastic analysis is presented in this article for a fully clamped beam struck transversely by a mass at any position on the span. The important influences of material strain rate sensitivity and finite deflections, as well as the effect of the transverse shear force on plastic yielding, are investigated. Good agreement is obtained between the present theoretical predictions for the maximum permanent transverse displacements and the previously published experimental results on both mild steel and aluminium alloy beams in Liu and Jones (1987) and Yu and Jones (1991). An energy density failure criterion, which was developed by Shen and Jones (1992), is examined for this particular problem which leads to some useful observations on the choice of the critical strain ε_c.

Acknowledgements—The authors wish to thank Dr C. E. Nicholson and the Health and Safety Executive at Sheffield for their support of this study through contract number 2516/R31.22. The authors are also indebted to the Impact Research Centre in the Department of Mechanical Engineering at the University of Liverpool and in particular to Mr F. J. Cummins for his assistance with the tracings.

REFERENCES

Jones, N. (1974). Some remarks on the strain-rate sensitive behaviour of shells. In *Problems of Plasticity* (Edited by A. Sawczuk), Vol. 2, pp. 403–407. Noordhoff, Gröningen.

Jones, N. (1989a). *Structural Impact*. Cambridge University Press, Cambridge, U.K.

Jones, N. (1989b). Some comments on the modelling of material properties for dynamic structural plasticity. In *Mechanical Properties of Materials at High Rates of Strain* (Edited by J. Harding), pp. 435–445. Institute of Physics, Bristol and New York.

Jones, N. (1989c). On the dynamic inelastic failure of beams. In *Structural Failure* (Edited by T. Wierzbicki and N. Jones), pp. 133–159. Wiley, New York.

Jones, N. and de Oliveira, J. G. (1979). The influence of rotatory inertia and transverse shear on the dynamic plastic behavior of beams. *J. Appl. Mech.* **46**(2), 303–310.

Liu, J. H. and Jones, N. (1987). Experimental investigation of clamped beams struck transversely by a mass. *Int. J. Impact Engng* **6**, 303–335.

Liu, J. H. and Jones, N. (1988). Dynamic response of a rigid plastic clamped beam struck by a mass at any point on the span. *Int. J. Solids Structures* **24**(3), 251–270.

Nonaka, T. (1967). Some interaction effects in a problem of plastic beam dynamics, parts 1–3. *J. Appl. Mech.* **34**, 623–643.

de Oliveira, J. G. (1982). Beams under lateral projectile impact. *Proc. ASCE, J. Engng Mech. Div.* **108** (EM1), 51–71.

Parkes, E. W. (1958). The permanent deformation of an encastré beam struck transversely at any point in its span. *Proc. Instn Civ. Engrs* **10**, 227–304.

Shen, W. Q. and Jones, N. (1991a). Interaction yield surfaces for the plastic behaviour of beams due to combined bending, tension and shear. Impact Research Centre Report No. ES/55/91. Dept. of Mech. Engng, University of Liverpool.

Shen, W. Q. and Jones, N. (1991b). A comment on the low speed impact of a clamped beam by a heavy striker. *Mech. Struct. Mach.* **19**(4), 527–549.

Shen, W. Q. and Jones, N. (1992). A failure criterion for beams under impulsive loading. *Int. J. Impact Engng* **12**(1), 101–121; **12**(2), 329.

Sobotka, Z. (1955). *Theorie Plasticity*. t.I-II, CSAV, Praha.

Symonds, P. S. (1965). Viscoplastic behaviour in response of structures to dynamic loading. In *Behaviour of Materials under Dynamic Loading* (Edited by N. J. Huffington), pp. 106–124. ASME, New York.

Yu, J. and Jones, N. (1991). Further experimental investigations on the failure of clamped beams under impact loads. *Int. J. Solids Structures* **27**(9), 1113–1137.